THE PROTEIN SOCIETY

Modulation of hemoglobin dynamics by an allosteric effector

Jyotsana Lal,[1]* Marco Maccarini,[2] Peter Fouquet,[2] Nancy T. Ho,[3] Chien Ho,[3] and Lee Makowski[1,4]

[1]Biosciences Division, Argonne National Laboratory, Argonne, Illinois 60439
[2]Institut Laue-Langevin, CS 20156, 38042 Grenoble Cedex 9, France
[3]Department of Biological Sciences, Carnegie Mellon University, Pittsburgh, Pennsylvania 15213
[4]Department of Bioengineering, Northeastern University, Boston, Massachusetts 02115

Received 1 October 2016; Accepted 7 December 2016
DOI: 10.1002/pro.3099
Published online 15 December 2016 proteinscience.org

Abstract: Hemoglobin (Hb) is an extensively studied paradigm of proteins that alter their function in response to allosteric effectors. Models of its action have been used as prototypes for structure-function relationships in many proteins, and models for the molecular basis of its function have been deeply studied and extensively argued. Recent reports suggest that dynamics may play an important role in its function. Relatively little is known about the slow, correlated motions of hemoglobin subunits in various structural states because experimental and computational strategies for their characterization are challenging. Allosteric effectors such as inositol hexaphosphate (IHP) bind to both deoxy-Hb and HbCO, albeit at different sites, leading to a lowered oxygen affinity. The manner in which these effectors impact oxygen binding is unclear and may involve changes in structure, dynamics or both. Here we use neutron spin echo measurements accompanied by wide-angle X-ray scattering to show that binding of IHP to HbCO results in an increase in the rate of coordinated motions of Hb subunits relative to one another with little if any change in large scale structure. This increase of large-scale dynamics seems to be coupled with a decrease in the average magnitude of higher frequency modes of individual residues. These observations indicate that enhanced dynamic motions contribute to the functional changes induced by IHP and suggest that they may be responsible for the lowered oxygen affinity triggered by these effectors.

Keywords: hemoglobin; protein dynamics; neutron spin echo; X-ray solution scattering

Jyotsana Lal current address is Physics Department, Boston University, Massachusetts 02215
Marco Maccarini current address is Laboratoire TIMC-IMAG, Université Grenoble Alpes, Grenoble, France

Grant sponsor: WAXS data was taken at BioCAT which is a National Institutes of Health-Supported Research Center; Grant number: RR08630; Grant sponsor: Use of Advanced Photon Source, an Office of Science User Facility Operated for the U.S. Department of Energy (DOE) Office of Science by Argonne National Laboratory, was supported by the U.S. DOE; Grant number: No. DE AC0206CH11357; Grant sponsor: C. Ho thanks National Institutes of Health for Support of Work on Hemoglobin; Grant number: R01GM084614.

*Correspondence to: J. Lal; E-mail: jlal@anl.gov

Introduction

Molecular models for hemoglobin (Hb) allostery are challenged by a vast literature of biochemical and biophysical results and, to some extent, no one model has proven capable of consistency with all available data. Studies of Hb in crystals or immobilized in gels[1–3] provide an opportunity to study intermediate states not accessible in solution, and could possibly discriminate among various models for allostery. But molecules, so constrained, do not exhibit dynamics on the time scales that occur in solution, and the potential impact of dynamics on function has not always been incorporated into the resultant models. The role that dynamics play in the cooperativity and regulation of oxygen binding to Hb has only recently

been appreciated.[4] Molecular dynamics studies[5] indicate an increased rate of molecular motions in deoxy-hemoglobin as compared to the liganded molecule. This seems paradoxical in view of the fact that HbCO A is much more likely to split into a pair of αβ-dimers than the deoxy form. Nuclear magnetic resonance (NMR) studies[6–8] paint a complex picture in which some residues become more rigid in the liganded state; whereas others gain flexibility in the deoxy form. Lower affinity states appear to exhibit greater structural flexibility than high affinity states.

The incorporation of dynamics into long-standing models for allostery has been hampered by lack of information on the impact that binding of ligands and allosteric effectors has on Hb dynamics. The prototypical view of Hb cooperativity is based on a stereochemical model[9] derived from low resolution crystallographic data. This model has graced virtually every biochemistry textbook for the past 40 years. Nevertheless, the discovery of alternate quaternary structures of hemoglobin[10–12] led to a reassessment of the molecular basis for its physiological responsiveness.[13] The average structure of liganded Hb appears intermediate between the R and R2 forms[14] where R2 is a liganded form of Hb that exhibits an arrangement of subunits almost as different from the prototypical R-state as the unliganded T-state.[13] Advances in computational and experimental tools created the opportunity to analyze differences in the dynamics of hemoglobin in different ligation states,[5,7,15] providing a basis for new models for Hb regulation.[4,5,16] Residual dipolar coupling (RDC) measurements of Hb A have shown that in solution the quaternary conformations of both the CO and the deoxy forms of Hb A are different from their crystal structures, and both exist as dynamic ensembles of various structures.[8,14,17,18] These results provide strong rationale for arguing that dynamics may play an important role in Hb allostery and function.

The importance of allosteric effectors on Hb function is well known.[19] Allosteric effectors such as 2,3 BPG and IHP bind to both the liganded and unliganded forms of Hb, albeit at different sites and resulting in different modulation of dynamics and function. The original X-ray crystallographic and model building results reported by Arnone and Perutz[20] suggested that 2,3-diphosphoglycerate (2,3-DPG) and IHP each bind to the central cavity of deoxy-Hb A[20,21] stabilizing the T-state quaternary structure, lowering the probability of a shift to the R-state and thereby lowering the affinity of Hb for oxygen.[20,21] The binding occurred at a 1:1 molar ratio near the entrance to the central cavity of Hb in a site that is occluded in the liganded form of Hb. No change in dynamic behavior was apparent on binding of IHP to deoxy-Hb,[7] but molecular dynamics (MD) simulations suggest an increase in intramolecular motions.[5]

These same effectors bind much more weakly to the liganded form of Hb,[22] but nevertheless, impact the structure and dynamics.[7,8,14,18] Arnone and coworkers[23] reported that no discrete IHP binding site(s) could be detected in the HbNO–IHP complex in their X-ray data. Based on gel filtration experiments, Gray and Gibson[22] reported that HbO_2 A can bind 1 or 2 molecules of IHP at pH 7 depending on the ionic strength of the media. More recently, it has been reported that binding is on the external surface, probably in the vicinity of αR141[7] and at a molar ratio of 2:1 effector to Hb[22] with the two binding sites separated by approximately 42 Å.[24] Ho and coworkers applied NMR relaxation techniques to demonstrate that the relaxation properties of a number of amino acid residues in HbCO A are affected by the presence of IHP.[7,25] They also applied NMR chemical shift perturbation and AUDO–DOCK methods to investigate the IHP binding sites of HbCO A,[25] finding that there are three likely IHP binding sites in HbCO A, namely (i) around the N-terminus and the C-terminus; (ii) around the EF loop; and (iii) in the $\alpha_1\beta_2$ interface around the switch region or αC helix-βFG corner and around the joint region or αFG corner-βC helix. These results may indicate that allosteric effectors, such as IHP alter dynamics of the Hb molecule, induce small changes in the tertiary and the quaternary structure of both deoxy- and CO-Hb while impacting ligand affinity.[14,17,18,25] Linking the changes in dynamics with changes in function is hampered by a major gap in our understanding of slow, coordinated motions, such as the rotation of αβ dimers relative to one another—a motion known to be important for function.

We have used neutron spin echo (NSE) to detect the motion of Hb αβ dimers relative to one another in solution.[26] These motions most likely follow functionally relevant pathways as observed for intramolecular motions of enzymes.[27] As such, they provide a window into the dynamics of conformational rearrangements required for allosteric control of oxygen binding. Here, we extend these earlier studies to characterize the impact of IHP binding on HbCO A dynamics. We demonstrate that IHP modulates the dynamics of HbCO A in the almost complete absence of structural change, and thereby suggest that changes in ligand affinity triggered by IHP are linked to alterations in dynamics.

Neutron spin-echo spectroscopy (NSE)[28] is a probe of protein dynamics sensitive to slow correlated motions (including translational and rotational diffusion and internal modes) on the picosecond to nanosecond time scale. NSE provides information about the time evolution of structural correlations analogous to dynamic light scattering but at time

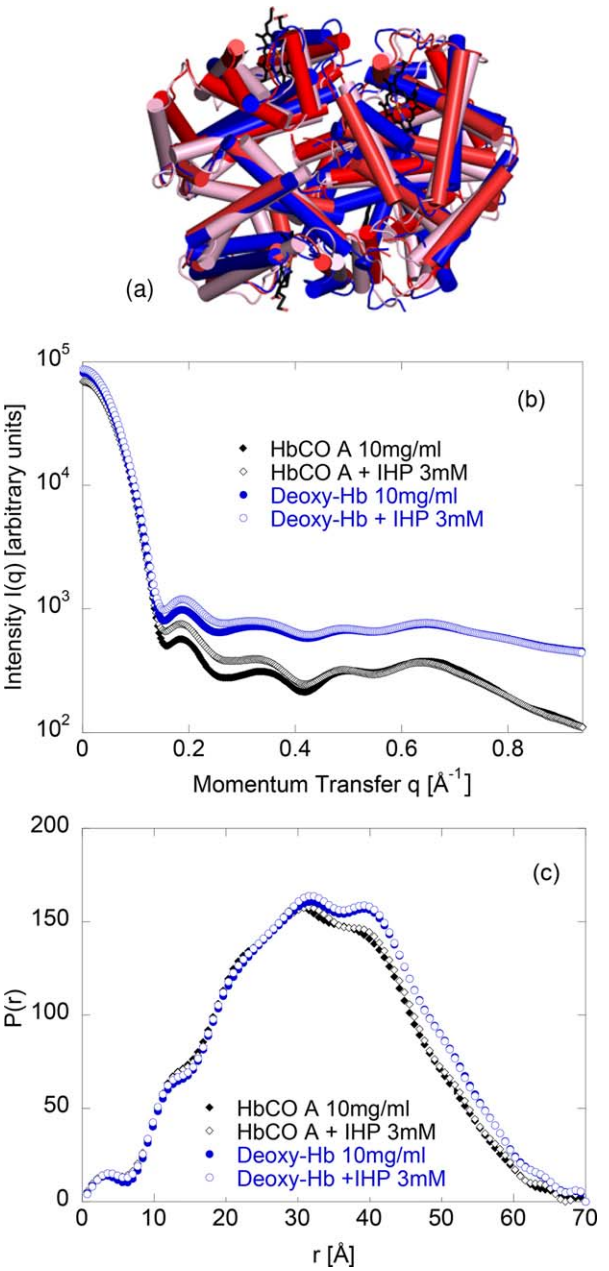

Figure 1. (A) The crystal structures. Shown for HbCO A (2DN3 red) human deoxy-Hb A (4HHB blue) and R2-state for liganded hemoglobin A (1BBB pink). Structures are aligned according to the α1β1 dimer. Figures were generated with the PyMOL program. (B) WAXS data. Shown for HbCO A, HbCO A + 3 m*M* IHP, deoxy Hb A and deoxy Hb A +3 m*M* IHP solutions taken at BioCAT at the APS. Deoxy Hb A WAXS data is slightly offset in y for a clearer display. The concentration of the proteins is 10 mg/mL. The intensity scale is arbitrary. (C) P(r) calculated from WAXS data. The calculation of p(r) in (C) are based on the measured WAXS data in (B).

and length scales more relevant to protein internal modes.[26,29–36] Recent NSE studies of Hb and myoglobin (Mb)[26] utilized data up to a very high momentum transfer q (~0.62 Å^{-1}) to characterize the internal dynamics of these proteins in terms of the dynamic pair correlation function and self-correlation function in the time range of several picoseconds to a few nanoseconds. This study established the effect of protein concentration and viscosity on decay times of internal modes. At relatively low protein concentrations, unexpectedly fast decay times at low q were interpreted in terms of the rotation of αβ dimers relative to one another. That study demonstrated that NSE can be used to simultaneously assess the effect of changes in protein environment on fast, small-scale motions of structural elements (from high q data) and the slower, correlated motions of subunits (from low q data). Here, we describe the application of this approach to study the effect of IHP binding on the internal dynamics of HbCO A.

Results

WAXS

The aligned crystal structures of HbCO A (2DN3 red) human deoxy-Hb A (4HHB blue) and R2-state for liganded hemoglobin A (1BBB pink) are superposed in Figure 1(A).

Examination of the wide angle X-ray scattering (WAXS) from HbCO A solutions provides a useful context in which to interpret the NSE data. The WAXS data provide a measure of the structural correlations that exist in HbCO A solution on the same length scale as NSE data. Figure 1(B) displays WAXS data collected from HbCO A, HbCO A +3 m*M* IHP, deoxy-Hb A, and deoxy Hb A +3 m*M* IHP using methods described previously.[37,38] The concentration of the proteins was 10 mg/mL. The position of the peak at 0.1875 Å^{-1} corresponds to interatomic vectors ~33 Å in length, roughly the center-to-center distance between subunits in the HbCO A tetramer. Data at momentum transfer $q \leq 0.3$ Å^{-1} (~20 Å spacing) represent quaternary structure features and $q \geq 0.3$ Å^{-1} corresponds to smaller distances representing tertiary and secondary structures. The peak at $q \sim 0.62$ Å^{-1} corresponds to interatomic vectors ~10 Å in length and is present in essentially all proteins with a large α-helical content because α-helices pack with a center-to-center distance of about 10 Å. Hemoglobin characteristically has a strong reflection at a scattering angle that corresponds to a 10 Å periodicity within the protein.[24]

In Figure 1(B), the WAXS curve show that IHP changes the scattering from both HbCO A and deoxy-Hb A in similar ways. The intensity differences associated with binding of IHP to HbCO A and deoxy-Hb A are consistent with a model in which there is little or no overall change in average structure. There is no change in the position of peaks. The radius of gyration R_g remains essentially constant within uncertainty although a small increase would be expected if—as predicted—the IHP were bound to the surface of the molecule.

Specifically, the estimates of R_g based on our data and calculated using GNOM[39] are: HbCO A = 24.65 Å, HbCO A + IHP = 24.79 Å, deoxy Hb A = 25.67 Å and deoxy Hb A + IHP = 25.60 Å. These numbers indicate that IHP does not alter R_g, consistent with essentially no change in structure on binding. They also compare well with the original measurements taken on human Hb[40] which were: deoxy Hb A − R_g = 26.2 Å; oxy Hb − R_g = 24.7 Å.

The WAXS data as reflected in the p(r) calculation in Figure 1(C) strengthens our argument that IHP alters the dynamics and not overall structure of both HbCO A and deoxy Hb A. The $p(r)$ are remarkably similar and indicate that there is essentially no detectable change in the structure of HbCO A and deoxy Hb A on IHP binding. This, in spite of the fact that the scattering is changed substantially [Fig. 1(B)]. The conclusion (similar to that observed in HIV protease[41]) is that dynamics are responsible for the majority of intensity change observed on IHP binding—and that the molecule is more flexible/dynamic when IHP binds.

The sum total of the WAXS results are that binding of IHP leads to changes in solution scattering that cannot be explained on the basis of structural change but are consistent with alterations expected in response to significant increases in the dynamics of the protein.

NSE

The NSE experiments carried out here provide measurements of the temporal development of the normalized structural correlation function $S(q,t)/S(q,0)$[28] in the range $t \sim 5$ ps to 28 ns. Data from HbCO A with and without IHP as well as matching buffers were collected over a range of q from 0.05 to 0.6 Å^{-1} at a protein concentration of 100 mg/mL and a temperature of 288 K. The signal of the buffer was eliminated during the data treatment by subtraction of the buffer signal as performed in our earlier studies.[26]

Polarization analysis was carried out at the beginning of data collection for all NSE spectra to determine the polarization and average signal for each detector. The detectors were grouped together with the same grouping used for the spectra, and the fractions of coherent and incoherent scattering as derived from the polarization analysis are plotted for HbCO A (± IHP) in deuterated water (D_2O) in Figure 2(A). At low q, the signal is largely coherent; at high q, the signal arises from mainly incoherent scattering. The transition point is at $q \sim 0.28$ Å^{-1}. The NSE data were measured in the same scattering wave vector range as the WAXS data in Figure 1(B). In the lower panel Figure 2(B) we show the level of incoherent and coherent scattering after subtraction of the buffer signal.

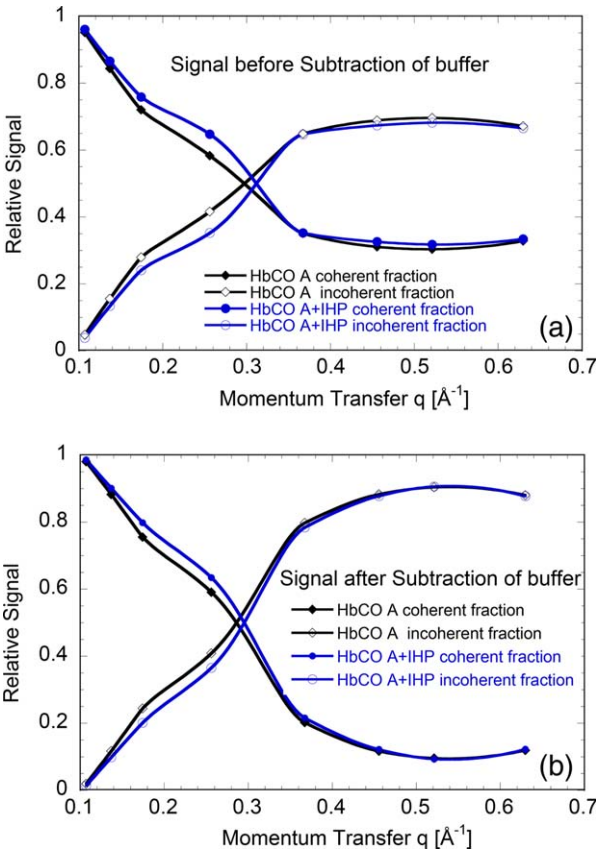

Figure 2. Polarization analysis. Shown for HbCO A (IHP) in solution in deuterated water (D_2O). The fractions of coherent and incoherent scattering are retrieved from the polarization analysis as a function of the scattering vector q. Measured with the NSE spectrometer IN11 (Institut Laue-Langevin). (a) Top panel displays the polarization analysis before subtraction of the D_2O buffer. (b) Bottom panel displays the polarization analysis after subtraction of the D_2O buffer.

At relatively small q, the NSE signal is dominated by coherent scattering and one measures the coherent correlation function $S^{coh}(q,t)$, which records the correlations of density fluctuations due to relative displacements $r_i - r_j$.

$$S^{coh} \cong \frac{1}{N}\sum_{ij} <e^{\left[-i\mathbf{q}\cdot\left(\mathbf{r}_i(0)-\mathbf{r}_j(t)\right)\right]}> \qquad (1)$$

where q is the momentum transfer, t denotes the time shift and i and j run over all atoms. N is the number of atoms in the ensemble.

Figures 3 and 4 include representative plots of $S(q,t)/S(q,0)$ for HbCO A measured at different qs. The data segregate into two classes (Figs. 3 and 4) that correspond to the degree of coherence in the scattering and clearly exhibit distinctive behaviors. The low q data (Fig. 3) exhibit relatively slow decay times and can be characterized in terms of a single exponential decay. At higher $q > 0.3$ Å^{-1} the coherent scattering contributes only modestly to the

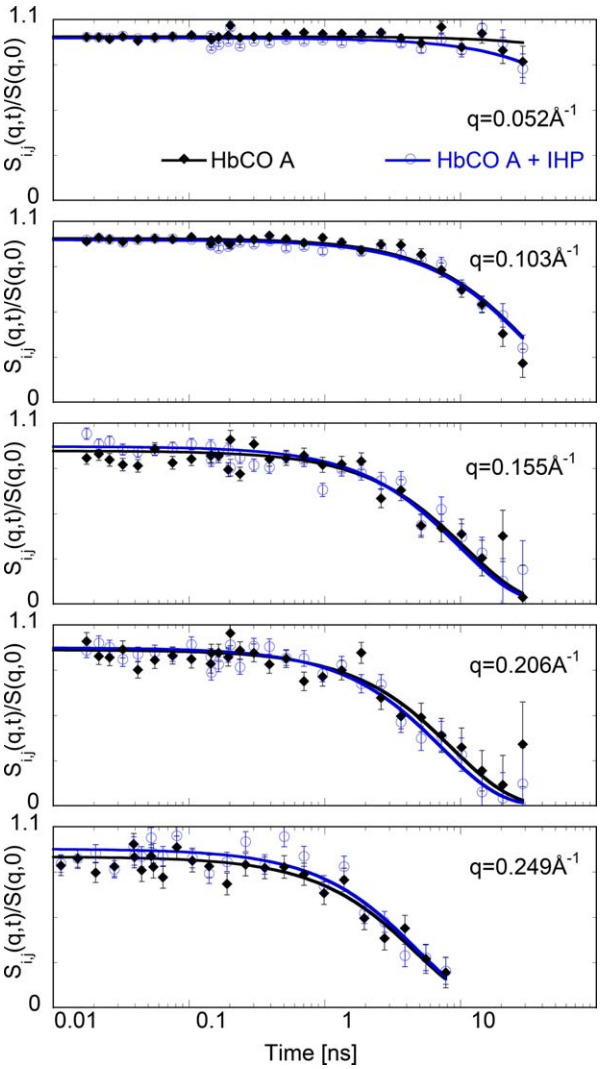

Figure 3. Coherent domain. Normalized structural correlation functions $S^{coh}(q,t)/S(q,0) = S_{ij}(q,t)/S(q,0)$ of HbCO A (IHP) in D_2O, as measured with the NSE spectrometer IN11 (Institut Laue-Langevin) at five momentum transfers q at a protein concentration of 100 mg/mL and a temperature of 288 K. Continuous lines indicate fits of the data to a single-exponential decay function.

signal (8–13%) and the spectra were analyzed as though due entirely to incoherent scattering (Fig. 4). The high q data are not consistent with a single exponential decay, but fit well to a 'stretched exponential function' without an elastic background level.

The data collected at $q < 0.3$ Å^{-1} and measured out to 28 ns are accurately fit using a single exponential, where

$$\frac{S^{coh}(q,t)}{S(q,0)} \cong e^{-\Gamma t} \quad (2)$$

Exponential fits resulted in estimation of the correlation times, $\tau = 1/\Gamma$, which are provided in Table I.

In this low q regime, IHP binding results in a statistically significant change in correlation time at $q \sim 0.2$ Å^{-1} (Table I, Figs. 3 and 5). This is the momentum transfer corresponding to the distance between subunits in HbCO A and in particular, to the $\alpha1-\beta2$ and $\alpha2-\beta1$ distances (~33 Å). At this value of momentum transfer, the scattering due to the quaternary structure of HbCO A has the largest contribution [cf. WAXS data Figure 1(B) and also Figure 6(A) from Ref. 26 for static neutron scattering measurements]. Correlation times at $q < 0.3$ Å^{-1} are consistent with translational, rigid body motion. However, it was previously shown[26] that in this q regime ($q < 0.3$ Å^{-1}) NSE observations should be interpreted as arising from a combination of translational and rotational diffusion, as well as subunit-subunit domain motion. It is unlikely that the binding of two IHP molecules (molecular weight 680 D each) would result in measurable changes in the rigid body motion of a 64 kDa molecular weight protein. Consequently, these data indicate that IHP binding increases the rate of motion of αβ-dimers relative to one another.

Furthermore, from the coherent intermediate scattering function $S^{coh}(q,t)$, one can extract a generalized time- and wavevector-dependent diffusion coefficient $D_{eff}(q)$ which corresponds to collective

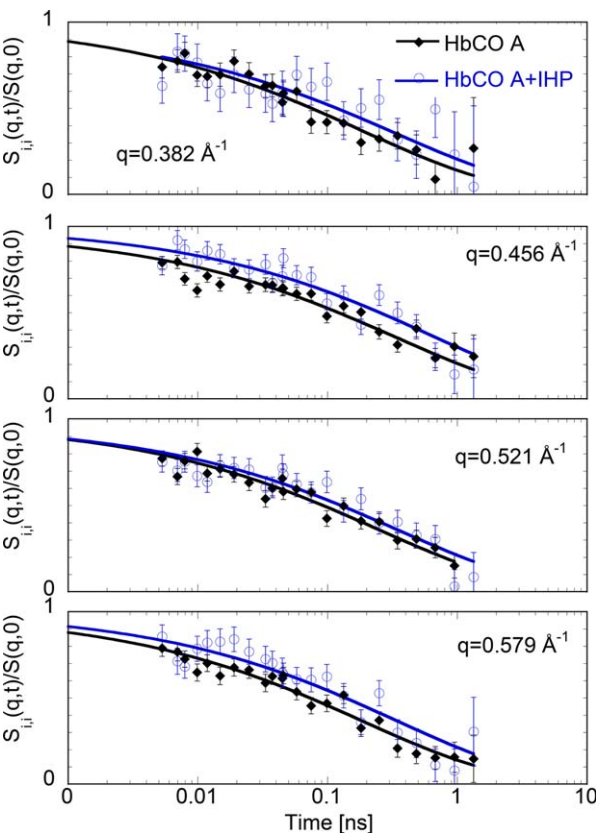

Figure 4. Incoherent domain. Normalized self correlation functions $S_{inc}(q,t)/S(q,0) = S_{ii}(q,t)/S(q,0)$ of HbCO A (IHP) in D_2O, as measured with the NSE spectrometer IN11 (Institut Laue-Langevin) at four momentum transfers q at a protein concentration of 100 mg/mL and a temperature of 288 K.

Table I. *Parameters from exponential fits*

	HbCO A				HbCO A +IHP			
q Å^{-1}	A	β	τ_{KWW} (ns)	$<\tau>$(ns)	A	β	τ_{KWW} (ns)	$<\tau>$(ns)
0.052	0.99	1.0	757.6	757.5 ± 925.4	0.98	1.0	174.8	174.8 ± 51.0
0.103	0.99	1.0	31.1	31.1 ± 2.5	0.98	1.0	31.0	31.0 ± 2.3
0.156	0.93	1.0	10.8	10.8 ± 1.2	0.96	1.0	9.8	9.8 ± 0.9
0.206	0.95	1.0	8.7	8.7 ± 1.1	0.96	1.0	7.3	7.3 ± 0.7
0.249	0.92	1.0	4.7	4.7 ± 0.5	0.97	1.0	4.7	4.7 ± 0.4
0.382	1.01	0.4	0.19	0.6 ± 0.1	0.97	0.4	0.34	1.1 ± 0.3
0.456	0.98	0.4	0.33	1.1 ± 0.1	1.01	0.4	0.63	2.1 ± 0.3
0.521	0.99	0.4	0.24	0.8 ± 0.1	0.98	0.4	0.35	1.2 ± 0.2
0.579	0.99	0.4	0.19	0.6 ± 0.1	1.01	0.4	0.33	1.1 ± 0.2

Characteristic time τ_{kww} (ns). Average relaxation time $<\tau> = \tau_{kww}/\beta\,\Gamma(1/\beta)$. Amplitude factors A. Stretch parameter β.

motion.[31] The relaxation rate, $\Gamma(q)$ [from Eq. (2)] and the effective diffusion constant, $D_{eff}(q)$, and correlation time, τ, are related as:

$$D_{\text{eff}}(q) = \frac{\Gamma(q)}{q^2} = \frac{1}{\tau q^2}. \quad (3)$$

The effective diffusion constant is thereby a measure of the decay rate of structural features with length scales corresponding to $2\pi/q$. $D_{eff}(q)$ has contributions from translational and rotational diffusion—both of which can be affected by interparticle interactions—as well as from internal modes of motion. The structural and hydrodynamic interactions are related by[26,31]

$$D_{\text{eff}}(q) = \frac{D^{o}_{\text{eff}}(q)H(q)}{S(q)} \quad (4)$$

where, $H(q)$ is the hydrodynamic function;[31] As described[34] however, for a protein, $D^{o}_{eff}(q)$ is the single particle effective diffusion constant. $S(q)$ is the structure factor of the protein in solution. $D_{eff}(q)$ is measurable from NSE, as indicated by Eq. (3). For the range of q examined in this study $H(q)$ appears to be nearly constant.[26]

Recently, this principle of de Gennes narrowing in Eq. (4) was also shown to hold for interdomain motion in several proteins.[35] Following this principle of de Gennes narrowing, the wavevector dependence of the interdomain diffusion coefficient $D_{eff}(q)$ is inversely proportional to the interdomain structure factor $S(q)$. In this case, $S(q)$ describes the relative spatial arrangement of domains within the protein.[35] This implies that the momentum transfer q at which structural (spatial) correlations due to domains are strong (narrow peak) the dynamics is slow. The WAXS data in Figure 1(b) shows that when IHP binds to HbCO A the static interdomain correlation peak at the momentum transfer q ~0.2 Å^{-1} (corresponding roughly to the center-to-center distance between subunits in the HbCO A tetramer) increases in width, that implies that as the spatial correlations become less strong and the

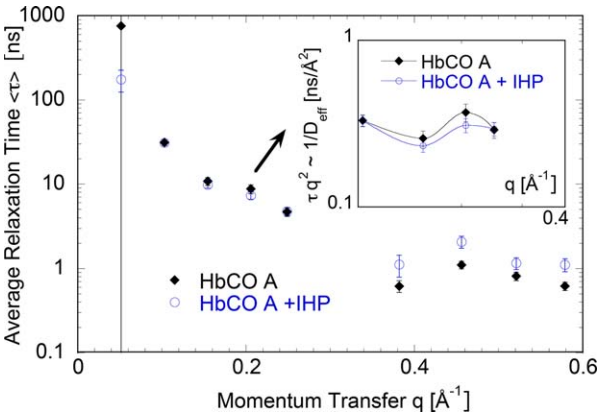

Figure 5. Relaxation times. Shown for both the coherent and incoherent domains. In the coherent scattering regime ($q < 0.3$ Å^{-1}), the relaxation time corresponds to that in Eq. (2), based on a single exponential fit (inset shows D_{eff} vs. q near 0.2 Å^{-1}) versus momentum transfer q. In the incoherent scattering regime ($q > 0.3$ Å^{-1}), the relaxation time corresponds to τ_{KWW} as defined in the discussion following Eq. (4) (Table I).

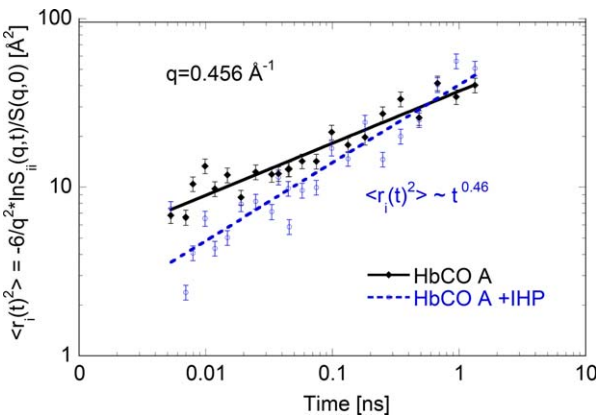

Figure 6. Root mean square displacement (RMSD) of hydrogens. RMSD of HbCO A and HbCO A + IHP solutions shown as a function of correlation time for the incoherent neutron scattering. For times less than about 1 ns, the RMSD is lower in the presence of IHP; for correlation times greater than a nanosecond, IHP induces an increase in RMSD.

dynamics at this q becomes faster as observed by a smaller τ in Figure 5 at the same q. The $D_{\text{eff}}(q)$ at this q is larger for HbCO A+ IHP than HbCO A alone [inset in Fig. 5 shows that $1/D_{\text{eff}}(q) \sim S(q)$ is broader for HbCO A + IHP than HbCO A; similar to the trend exhibited by the WAXS data in Fig. 1(B)]. The changes observed in D_{eff} should be dominated by motion of αβ-dimers relative to one another as the rigid body motions on binding of a small IHP to HbCO A should not change.

WAXS data reinforces the coherent $S^{\text{coh}}(q,t)$ interdomain NSE results quite precisely. This principle of de Gennes narrowing for interdomain motion has been demonstrated for several proteins recently.[31–33] In our case too, the wave vector dependence of the interdomain diffusion coefficient is inversely proportional to the interdomain structure factor. Changes in the interdomain diffusion coefficient and interdomain structure factor observed on IHP binding are consistent with the principle of de Gennes narrowing.

At larger q, the signal is dominated by incoherent scattering by hydrogens (within the protein, since solvent is 100% D_2O) and one measures the incoherent or self correlation function,

$$S^{\text{inc}} \cong < e^{[-i\boldsymbol{q}\cdot(\boldsymbol{r}_i(0)-\boldsymbol{r}_i(t))]} > \tag{5}$$

In this range, the $S^{\text{inc}}(q,t)$ data (measured out to 1.4 ns) cannot be accurately fit with a single exponential decay function. They do, however, fit well to a 'stretched' exponential[42,43] of the form:

$$\frac{S^{\text{inc}}(q,t)}{S(q,0)} \cong e^{-(\Gamma t)^{\beta}} \tag{6}$$

as shown in Figure 4. The processes giving rise to the data at $q > 0.30$ Å^{-1} are the self motion of hydrogens within the protein. Analysis of predicted quasi-elastic neutron scattering data from MD simulations indicates that the stretch factor $\beta(q)$ reaches a constant value for large q in the range of 0.2–0.5 Å^{-1}, with the specific value dependent on the nature of the atoms contributing (e.g., main chain; side chain). Our observations are consistent with these predictions and derive an excellent fit to the stretched exponential with $\beta = 0.4$ and $\Gamma = 1/\tau_{\text{KWW}}$ (see Table I), where τ_{KWW} is the Kohlrausch–William–Watts characteristic time.[43] The characteristic times estimated from the stretched–exponential fits represent an average over all hydrogens in the protein.

As can be seen in Figures 4 and 5 (at $q > 0.3$ Å^{-1}, Table I), IHP binding appears to result in a modest suppression of the average self motion of the hydrogens in the protein. This result would seem inconsistent with a simultaneous decrease in the correlation times observed at $q \sim 0.2$ Å^{-1} and attributable to faster dimer–dimer rotation dynamics. But these two observations need not be mutually exclusive. First, in the case of the wide angle measurements, we observe an average correlation time. This might include, for instance, increased correlation times for hydrogens in direct contact with the binding IHP molecule, but decreased times for hydrogens at the α1β2 and α2β1 interfaces. Second, the slowing appears to be associated with very short correlation times (<1 ns). To demonstrate this, we used the curves in Figure 4 to calculate the average root mean square displacement (RMSD) of these hydrogens as a function of correlation time. As shown in Figure 6, the RMSD decreases in response to IHP binding for correlation times less than a nanosecond, and increases upon IHP binding for longer correlation times. This is consistent both with the pair correlation observations made at low q by NSE and the estimates of ensemble breadth based on WAXS data. The blue line in Figure 6 shows that RMSD on IHP binding can be described by a power law with an exponent of 0.46 which indicates that the motion for the hydrogens is subdiffusive.

Discussion

NMR studies of IHP binding to HbCO A[7] indicate that some residues, such as α40Lys become more rigid on IHP binding. Those same studies[7] indicate that several amino acid residues at the interdimer (α1β2 or α2β1) interface exhibit significant conformational exchange in response to IHP binding. The affected residues include the proximal β92His in the β-heme pocket, and residues located in the flexible joint (βC helix-αFG corner) and switch (αC helix-βFG corner) regions that play an important role in the dimer–dimer rotation of Hb during the oxygenation process. Our observations of enhanced dynamics at a wavevector q corresponding to the distance between α1β2 and α2β1 subunits suggests that the increased dynamics at these interfaces observed by NMR is associated with extensive motion of the αβ-dimers relative to one another.

Cammarata *et al.*[44,45] collected time-resolved WAXS (tr-WAXS) data from Hb as little as 200 nsec after laser photolysis. This corresponds to the slowest processes accessible to NSE and, in NSE data is confounded by diffusive motion of the entire molecules. The inter-subunit motions detected here by NSE occur at time frames not yet reached by tr-WAXS. Conformational changes involved in switching from low-affinity deoxy to high affinity liganded structures typically are much slower than the motions observable by NSE. Nevertheless, the coupling of slow and fast dynamics is becoming a common theme in protein function at different length and time scales. Here, we show that the motion of αβ dimers relative to one another in the Hb

tetramer is modulated by IHP binding in the absence of a gross re-arrangement of quaternary structure.

The picture that emerges from these measurements suggests increased dynamics at the level of quaternary structure and the residues involved in dimer-dimer interactions, coupled with a modest increase in the rigidity of individual subunits. The correspondence of increased structural fluctuations with decreased oxygen affinity is a theme that has received substantial support recently.[5] The NSE measurements reported here provide strong additional evidence of this pattern of response to allosteric effectors.

The theory of conformational selection indicates that a protein undergoes structural fluctuations in solution and that only a sub-set of those conformations are capable of binding to a specific ligand. The more dynamic the protein, the smaller the proportion of conformations capable of binding. Consequently, enhanced dynamics may often be associated with decreased affinity.[46]

In conclusion, NSE measurements demonstrate that, on average, IHP induces an increase in the rate of coordinated motions of Hb subunits relative to one another. This is coupled with a decrease in the average magnitude of higher frequency modes of individual residues. The $D_{eff}(q)$ inferred from the coherent intermediate scattering function measured by NSE possesses an inverse q dependence on the interdomain structure factor measured by WAXS. The principle of de Gennes narrowing explains faster dynamics at $0.2 Å^{-1}$ on binding of IHP (inter domain S(q) in the WAXS data shows a broadening also the $D_{eff}(q)$ is larger), relative to HbCO A alone (interdomain S(q) in the WAXS data is narrower and also $D_{eff}(q)$ is smaller). The changes observed in $D_{eff}(q)$ should be dominated by motion of αβ-dimers relative to one another as the rigid body motions on binding of a small IHP to HbCO A should not change. The principle of de Gennes narrowing supports this interpretation of changes in the relative inter-domain motion of a protein on binding of a small molecule.

These results indicate that NSE has great potential for studying the dynamics and interactions of macromolecular systems in solution close to physiological conditions. We have chosen a well-studied system, i.e., hemoglobin and its interactions with allosteric effector, to test the power of NSE. Our NSE results are consistent with published NMR and WAXS results on hemoglobin and hemoglobin + IHP interactions. This suggests that NSE methodology can be applied together with other complementary techniques to study structures and dynamics of other important, complex macromolecular systems.

Materials and Methods

NSE is a very high-resolution neutron scattering technique where we measure up to sub-neV energy transfer between the probe and the sample nuclei. The energy transfer is encoded in the change of spin precession angle of the neutrons which is measured as change of polarization at the detector. This energy transfer can be related to various correlation functions from the sample and here the structural correlation function $S(q,t)$ is measured. In our previous paper[26] we developed the methodology to measure motion (from two different nuclei) scattering at different times to measure collective coordinated motion of protein subunits at low momentum transfer and measure self local motion (from same nuclei) at different times at large momentum transfer in the same experiment. The self local motion is measurable because of the large incoherent hydrogen scattering cross-section from the protein dominates the signal at large momentum transfer. During NSE experiments, a sample of D_2O salt buffer is measured with equal statistics, which allows us to subtract the signal of the buffer in the experimental analysis. Through these high resolution X-ray and neutron scattering experiments both spatial and dynamic correlations of intramolecular motions of protein molecules are measurable in solution.

Wide-angle X-ray scattering (WAXS) data were collected at the BioCAT undulator beam line (18ID)[47] at the Advanced Photon Source (APS), Argonne, IL, USA using methods previously described in detail.[37,38] Rg and P(r) were calculated using the program GNOM.[39] The experiments on protein dynamics were performed at the NSE spectrometer IN11 at the Institute Laue Langevin, Grenoble, France, using a wavelength of 5.5 Å and the high intensity 30 degree detector option IN11C for the high q data. For the low q data we used a wavelength of 8.5 Å and the high resolution detector of IN11A. The correlation function $S(q,t)$ as function of time, t was measured over a time range from 0.005 to 28 ns and a momentum transfer range from 0.10 to $0.65 Å^{-1}$.

The first sample was about 3 mL of HbCO A solution, at a concentration of about 100 mg/mL in 50 m*M* sodium phosphate at pH 7.1 in heavy water (D_2O). Subtraction was done with the matching buffer for the sample. The second sample was about 3 mL of HbCO A solution, at a concentration of about 100 mg/mL in 50 m*M* sodium phosphate at pH 7.1 in D_2O and 3 m*M* IHP. Again, subtraction was done with the matching buffer for the sample. The samples were measured at a temperature of 288 K.

Acknowledgments

We want to thank Yue Yuan from University of Notre Dame for providing help with Figure 1(a) in this paper. We also acknowledge the provision of neutron beam time by Institute Laue Langevin, Grenoble, France.

References

1. Jones EM, Balakrishnan G, Spiro TG (2012) Heme reactivity is uncoupled from quaternary structure in gel-capsulated hemoglobin: A resonance Raman spectroscopic study. J Am Chem Soc 134:3461–3471.
2. Jones EM, Monza E, Balakrishnan G, Blouin GC, Mak PJ, Zhu Q, Kincaid JR, Guallar V, Spiro TG (2014) Differential control of heme reactivity in alpha and beta subunits of hemoglobin: a combined Raman spectroscopic and computational study. J Am Chem Soc 136: 10325–10339.
3. Henry ER, Mozzarelli A, Viappiani C, Abbruzzetti S, Bettati S, Ronda L, Bruno S, Eaton WA (2015) Experiments on hemoglobin in single crystals and silica gels distinguish among allosteric models. Biophys J 109: 1264–1272.
4. Yuan Y, Tam MF, Simplaceanu V, Ho C (2015) New look at hemoglobin. Allostery Chem Rev 115:1702–1724.
5. Yonetani T, Laberge M (2008) Protein dynamics explain the allosteric behaviors of hemoglobin. Biochim Biophys Acta 1784:1146–1158.
6. Song XJ, Yuan Y, Simplaceanu V, Sahu SC, Ho NT, Ho C (2007) A comparative NMR study of the polypeptide backbone dynamics of hemoglobin in the deoxy and carbonmonoxy forms. Biochemistry 46:6795–6803.
7. Song XJ, Simplaceanu V, Ho NT, Ho C (2008) Effector-induced structural fluctuation regulates the ligand affinity of an allosteric protein: binding of inositol hexaphosphate has distinct dynamic consequences for the T and R states of hemoglobin. Biochemistry 47:4907–4915.
8. Lukin JA, Kontaxis G, Simplaceanu V, Yuan Y, Bax A, Ho C (2003) Quaternary structure of hemoglobin in solution. Proc Natl Acad Sci USA 100:517–520.
9. Perutz MF (1970) Stereochemistry of cooperative effects in haemoglobin. Nature 228:726–739.
10. Smith FR, Lattman EE, Carter CW, Jr. (1991) The mutation β99 Asp-Tyr stabilizes Y—a new composite quaternary state of human hemoglobin. Proteins 10: 81–91.
11. Mueser TC, Rogers PH, Arnone A (2000) Interface sliding as illustrated by the multiple quaternary structures of liganded hemoglobin. Biochemistry 39:15353–15364.
12. Kavanaugh JS, Rogers PH, Arnone A (2005) Crystallographic evidence for a new ensemble of ligand-induced allosteric transitions in hemoglobin: the T-to-T(high) quaternary transitions. Biochemistry 44:6101–6121.
13. Tame JRH (1999) What is the true structure of liganded haemoglobin? Trends Biochem Sci 24:372–377.
14. Gong Q, Simplaceanu V, Lukin JA, Giovannelli JL, Ho NT, Ho C (2006) Quaternary structure of carbonmonoxyhemoglobins in solution: structural changes induced by the allosteric effector inositol hexaphosphate. Biochemistry 45:5140–5148.
15. Yuan Y, Simplaceanu V, Lukin JA, Ho C (2002) NMR investigation of the dynamics of tryptophan side-chains in hemoglobins. J Mol Biol 321:863–878.
16. Yonetani T, Park S, Tsuneshige A, Imai K, Kanaori K (2002) Global allostery model of hemoglobin—modulation of O_2-affinity, cooperativity, and Bohr effect by heterotropic allosteric effectors. J Biol Chem 277: 34508–34520.
17. Sahu SC, Simplaceanu V, Ho NT, Giovannelli JL, Ho C (2006) Backbone resonance assignment of human adult hemoglobin in the deoxy form. J Biomol NMR 36:1–1.
18. Sahu SC, Simplaceanu V, Gong Q, Ho NT, Tian F, Prestegard JH, Ho C (2007) Insights into the solution structure of human deoxyhemoglobin in the absence and presence of an allosteric effector. Biochemistry 46: 9973–9980.
19. Benesch R, Benesch RE (1967) The effect of organic phosphates from the human erythrocyte on the allosteric properties of hemoglobin. Biochem Biophys Res Commun 26:162–167.
20. Arnone A, Perutz MF (1974) Structure of inositol hexaphosphate–human deoxyhaemoglobin complex. Nature 249:34–36.
21. Arnone A (1972) X-ray diffraction study of binding of 2,3-diphosphoglycerate to human deoxyhaemoglobin. Nature 237:146–149.
22. Gray RD, Gibson QH (1971) The effect of inositol hexaphosphate on the kinetics of CO and O_2 binding by human hemoglobin. J Biol Chem 246:7168–7174.
23. Chan N-L, Kavanaugh JS, Rogers PH, Arnone A (2004) Crystallographic analysis of the interaction of nitric oxide with quaternary-T human hemoglobin. Biochemistry 43:118–132.
24. Makowski L, Bardhan J, Fischetti Gore RD, Lal J, Mandava S, Park S, Rodi DJ, Ho NT, Ho C (2011) WAXS studies of the structural diversity of hemoglobin in solution. J Mol Biol 408:909–921.
25. Fan JS, Zheng Y, Choy WY, Simplaceanu V, Ho NT, Ho C, Yang DI (2013) Solution structure and dynamics of human hemoglobin in the carbonmonoxy form. Biochemistry 52:5809–5820.
26. Lal J, Fouquet P, Maccarini M, Makowski L (2010) Neutron spin echo studies of hemoglobin and myoglobin: multiscale internal dynamics. J Mol Biol 397:423–435.
27. Henzler-Wildman K, Kern D (2007) Dynamic personalities of proteins. Nature 450:06522.
28. Mezei F (1980) Neutron spin echo (Lecture Notes in Physics), Vol. 128. Berlin: Springer.
29. Bu Z, Biehl R, Monkenbusch M, Richter D, Callaway DJE (2005) Coupled protein domain motion in *Taq* polymerase revealed by neutron spin-echo spectroscopy. Proc Natl Acad Sci USA 102:17646–17651.
30. Doster W, Longeville S (2007) Microscopic diffusion and hydrodynamic interactions of hemoglobin in red blood cells. Biophys J 93:1360–1368.
31. Biehl R, Hoffmann B, Monkenbusch M, Falus P, Preost S, Merkel R, Richter D (2008) Direct observation of correlated interdomain motion in alcohol dehydrogenase. Phys Rev Lett 101:138102–138104.
32. Farago B, Li J, Cornilescu G, Callaway DJE, Bu Z (2010) Activation of nanoscale allosteric protein domain motion revealed by neutron spin echo spectroscopy. Biophys J 99:3473–3482.
33. Wang S-C, Mirarefi P, Faraone A, Lee CT Jr. (2011) Light-controlled protein dynamics observed with neutron spin echo measurements. Biochemistry 50:8150–8162.
34. Biehl R, Monkenbusch M, Richter D (2011) Exploring internal protein dynamics by neutron spin echo spectroscopy. Soft Matter 7:1299–1307.
35. Hong L, Smolin N, Smith JC (2014) de Gennes narrowing describes the relative motion of protein domains. Phys Rev Lett 112:158102–158104.
36. Grimaldo M, Roosen-Runge F, Jalarvo N, Zamponi M, Zanini F, Hennig M, Zhang F, Schreiber F, Seydel T (2015) High-resolution neutron spectroscopy on protein solution samples. EPJ 83:02005–02006.
37. Makowski L, Rodi DJ, Mandava S, Minh D, Gore D, Fischetti RF (2008) Molecular crowding inhibits intramolecular breathing motions in proteins. J Mol Biol 375:529–546.

38. Makowski L (2010) Characterization of proteins with wide-angle X-ray solution scattering (WAXS). J Struct Funct Genomics 11:9–19.
39. Svergun DI (1992) Determination of the regularization parameter in indirect-transform methods using perceptual criteria. J Appl Crystallogr 25:495–503.
40. Conrad H, Mayer A, Thomas HP, Vogel H (1969) X-ray small-angle scattering from aqueous solutions of oxy- and deoxyhaemoglobin. J Mol Biol 41:225–229.
41. Zhou H, Li S, Badger J, Nalivaika E, Cai Y, Foulkes-Murzycki J, Schiffer C, Makowski L (2015) Modulation of HIV protease flexibility by the T80N mutation. Proteins 83:1929–1939.
42. Glockle WG, Nonnenmacher TF (1995) A fractional calculus approach to self-similar protein dynamics. Biophys J 68:46–53.
43. Dellerue S, Petrescu A-J, Smith JC, Bellissent-Funel MC (2001) Radially softening diffusive motions in a globular protein. Biophys J 81:1666–1676.
44. Cammarata M, Levantino M, Schotte F, Anfinrud PA, Ewald F, Choi J, Cupane A, Wulff M, Ihee H (2008) Tracking the structural dynamics of proteins in solution using time-resolved wide-angle X-ray scattering. Nat Methods 5:881–886.
45. Cammarata M, Levantino M, Wulff W, Cupane A (2010) Unveiling the timescale of the R–T transition in human hemoglobin. J Mol Biol 400:951–962.
46. Csermely P, Palotai R, Nussinov R (2010) Induced fit, conformational selection and independent dynamic segments: an extended view of binding events. Trends Biochem Sci 35:539–546.
47. Fischetti RF, Stepanov S, Rosenbaum G, Barrea R, Black E, Gore D, Heurich R, Kondrashkina E, Kropf AJ, Wang S, Zhang K, Irving TC, Bunker GB (2004) The BioCAT undulator beamline 18ID: a facility for biological non-crystalline diffraction and X-ray absorption spectroscopy at the advanced photon source. J Synchrotron Radiat 11:399–405.